Figure S1. Observed (blue) and modelled (red) tidally averaged salinity time series for the year 2022 for different observation stations in the Rhine-Meuse Delta. Locations of the stations are indicated in Fig. 1 in the main text.
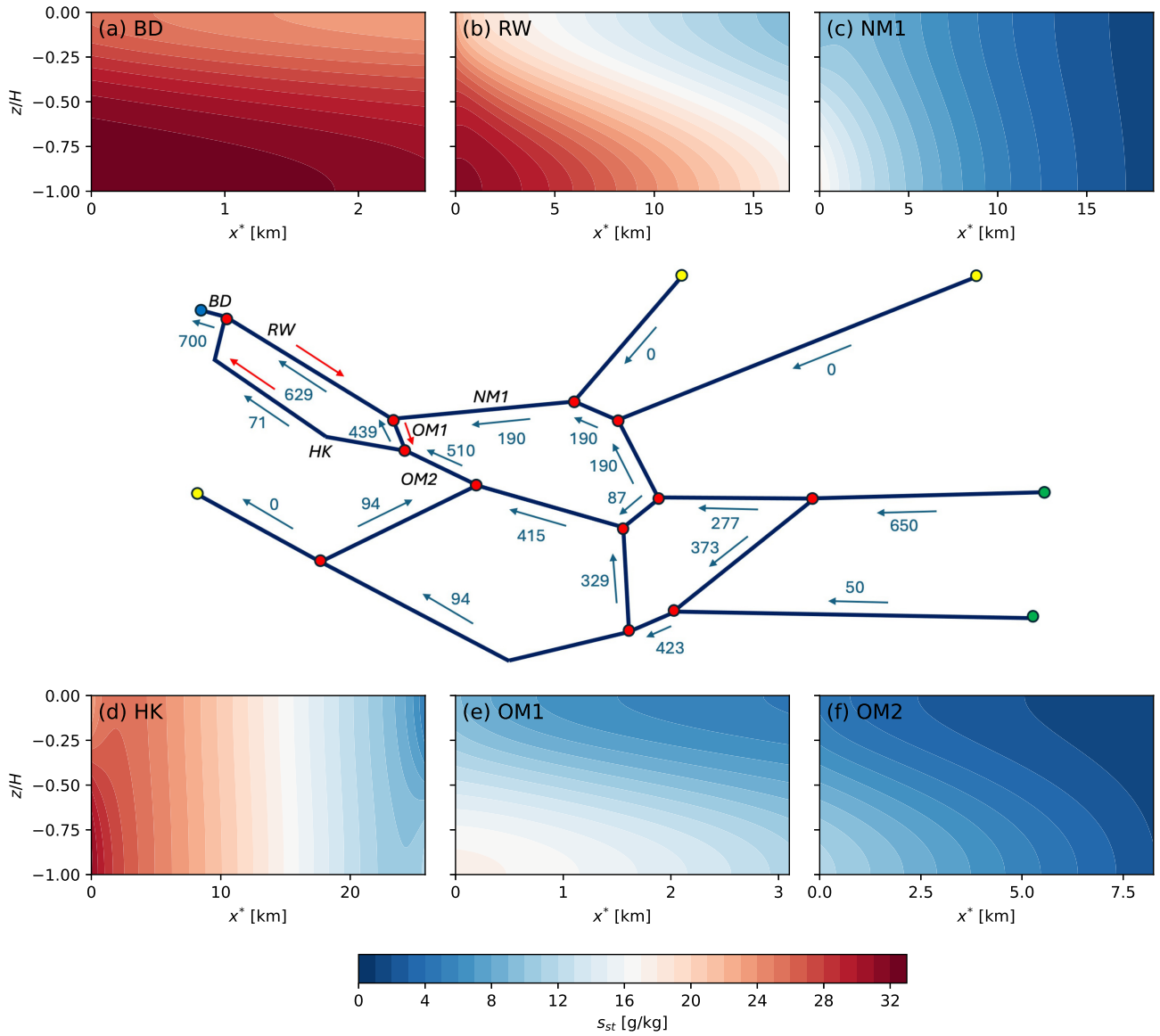
Figure S2. Center panel: As Fig. 2a in the main text, but with the discharge distribution in the Rhine-Meuse Delta for low flow conditions. Values are in m^3s^{-1}. The red arrows indicate the direction of net salt transport (overspill). (a)-(f) Subtidal salinities under low flow conditions as a function of $x^* \equiv -x$, and $\frac{z}{H}$ for different channels.
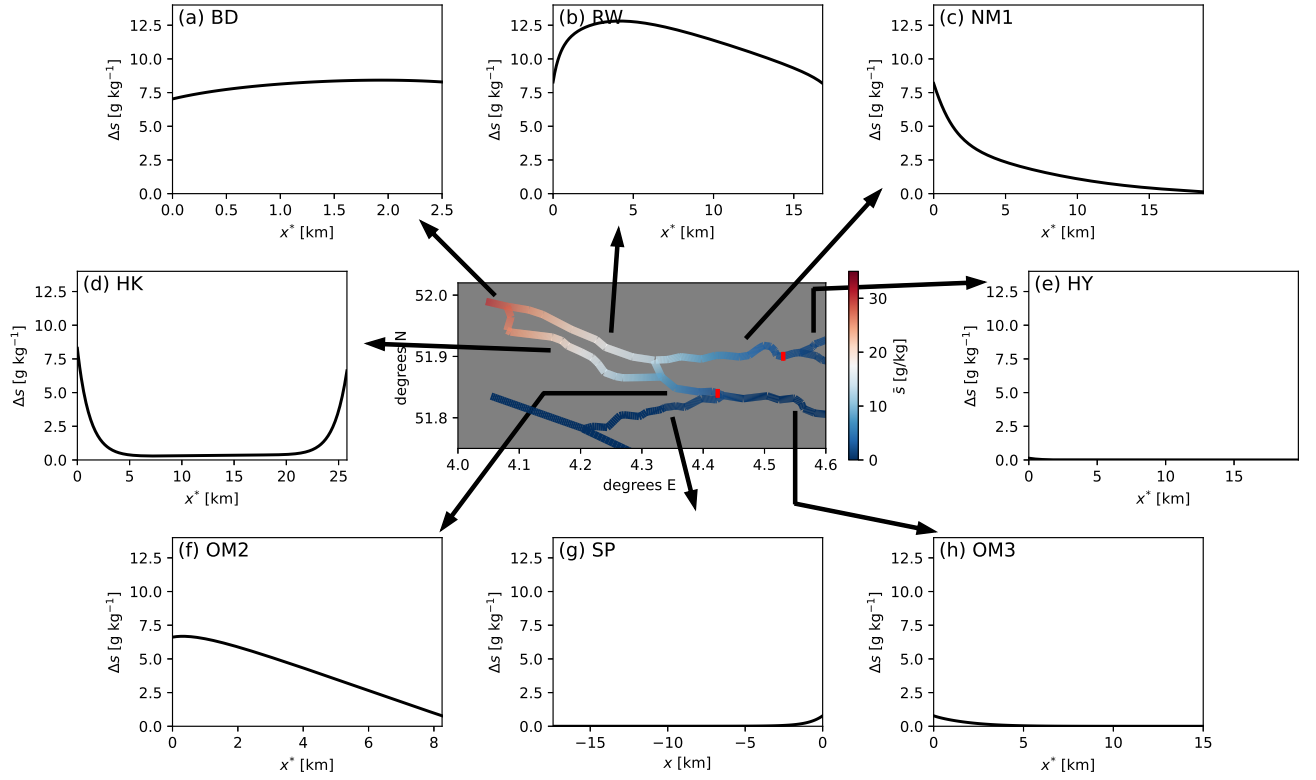
Figure S3. Center panel: depth and tidally averaged salinity in the Rhine-Meuse Delta for low discharge conditions. The red lines in this figure indicate the location of the 2 g kg^{-1} isohaline. (a)-(h) Surface-bottom subtidal salinity difference, versus x or $x^* \equiv -x$ for different channels.
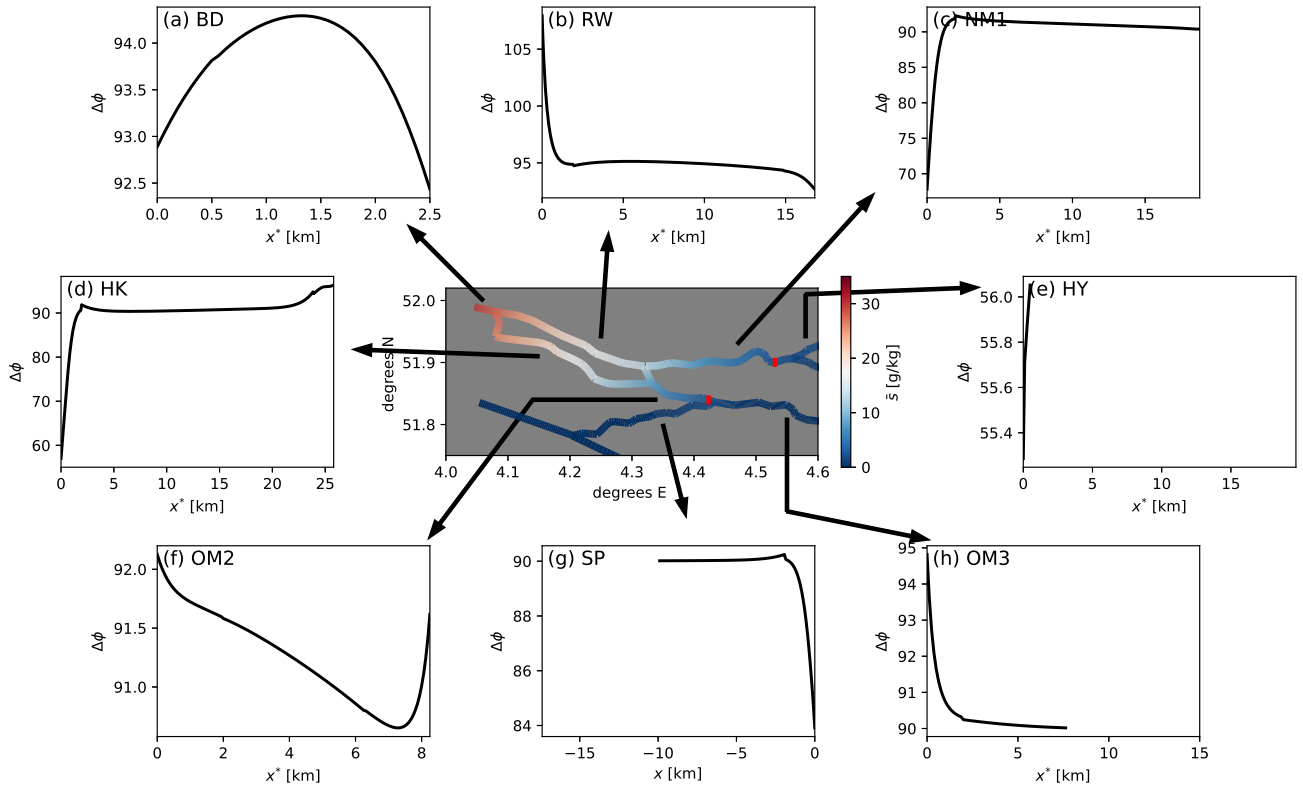
Figure S4. Center panel: depth and tidally averaged salinity in the Rhine-Meuse DeltaMD for low discharge conditions. The red lines in this figure indicate the location of the 2 g kg^{-1} isohaline. (a)-(h) Phase difference between depth-averaged tidal current and salinity $\Delta\phi$, versus x or $x^* \equiv -x$ for different channels.
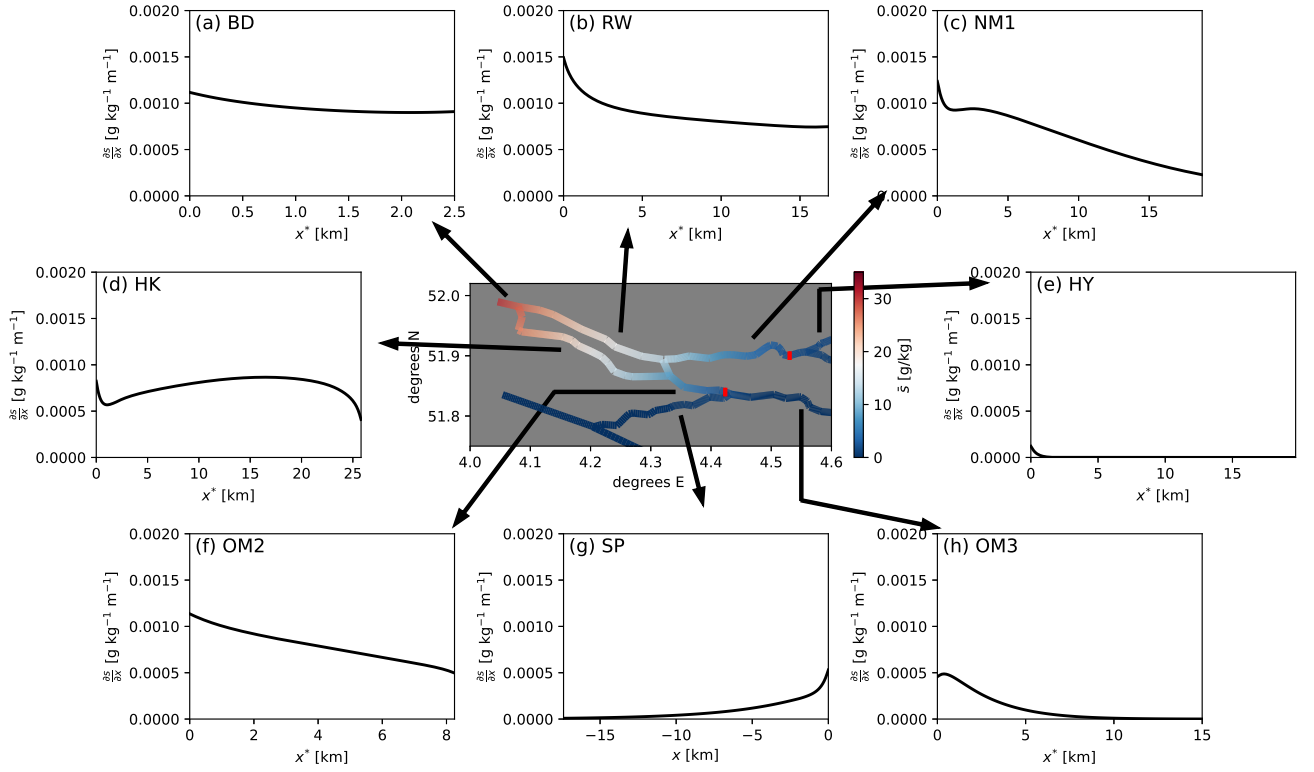
Figure S5. Center panel: depth and tidally averaged salinity in the Rhine-Meuse Delta for low discharge conditions. The red lines in this figure indicate the location of the 2 g kg^{-1} isohaline. (a)-(h) Horizontal gradient of the subtidal salinity, versus x or $x^* \equiv -x$ for different channels.